Proceedings of the XVII ECSMGE-2019
Geotechnical Engineering foundation of the future
ISBN 978-9935-9436-1-3

doi: 10.32075/17ECSMGE-2019-0408

XVII European Conference
ECSMGE 2019
Reykjavik
on Soil Mechanics
and Geotechnical Engineering

Numerical analysis of cavity propagation in deep trapdoor experiments

Analyse numérique de la propagation de cavités dans des expériences de trappes profondes

A. S. Osman
Durham University, Durham, UK

S. W. Jacobsz, C. Purchase
University of Pretoria, Pretoria, South Africa

ABSTRACT: Large areas of the economically important Gauteng Province of South Africa are underlain by extensively weathered dolomite bedrock in which sinkholes are a common occurrence. Deep trapdoor experiments were conducted in the geotechnical centrifuge to study cavity propagation towards the surface to obtain a better understanding of the sinkhole development process and the factors affecting it. The experimental programme is accompanied by a numerical modelling programme in order to gain better understanding on the behaviour of cavity propagation above trapdoors. A series of finite element simulations were carried out using the Coupled Eulerian–Lagrangian (CEL) method. It was found that in deep trapdoors, shear bands initiate from the edges of the trapdoor, propagating upwards. The bands curve inwards under the influence of the mobilised dilation angle which depends on the stress level and relative density of the placed soil. With large trapdoor movement, near vertical shear zones develop. These results imply that the guidelines for the assessment of sinkhole size in South Africa are conservative and there is room for improving the current guidelines by adopting realistic mechanisms of sinkhole development.

RÉSUMÉ:
Vastes zones de la province économiquement importante de Gauteng en Afrique du Sud reposent sur un substrat rocheux dolomitique fortement altéré, dans lequel des gouffres sont fréquents. Des expériences de trappes profondes ont été menées dans la centrifugeuse géotechnique afin d'étudier la propagation de la cavité vers la surface afin de mieux comprendre le processus de développement du puisard et ses facteurs. Le programme expérimental est accompagné d'un programme de modélisation numérique pour mieux comprendre le comportement de la propagation de la cavité au-dessus des trappes. Une série de simulations avec des éléments finis a été réalisée à l'aide de la méthode Coupled Eulerian – Lagrangian (CEL). Il a été constaté que, dans les trappes profondes, des bandes de cisaillement s'initient à partir des bords de la trappe, se propageant vers le haut. Les bandes se courbent vers l'intérieur sous l'influence de l'angle de dilatation mobilisé qui dépend du niveau de contrainte et de la densité relative du sol appliqué. Avec de grands mouvements de trappe, des zones de cisaillement presque verticales se développent. Ces résultats impliquent que les directives pour l'évaluation de la taille des gouffres en Afrique du Sud sont conservative et qu'il est encore possible d'améliorer les directives actuelles en adoptant des mécanismes réalistes de développement des gouffres.

Keywords: trapdoor, sand, finite element, Coupled Eulerian Lagrangian.

1 INTRODUCTION

Loss of ground support can result from a variety of activities such tunnelling, mining, erosion due to leaking services, poor compaction and due to karstic sub-soil conditions (Costa et al., 2009). In certain instances, the loss of ground support is amenable to be modelled by means of trapdoor experiments. Several studies are available in the literature investigating the response of sand above active trapdoors (e.g. Terzaghi 1936; Koutsabeloulis and Griffiths 1989; Stone and Muir Wood 1992). Most of the available studies have been carried out on shallow trapdoors, i.e. experiments in which the H/B (soil height/trapdoor width) ratio is less than two (Costa et al., 2009). Although limited work has been carried out on deep trapdoors, the focus has generally been on the load on the trapdoor. Limited information is available on the mechanism of propagation of the zone of influence above deep trapdoors. In addition, the displacements of trapdoors reported in the literature were generally small, with limited information being available on the propagation of the zone of influence due to large trapdoor displacements.

2 CENTRIFUGE MODELS

A series of deep trapdoor experiments were carried out in the geotechnical centrifuge of the University of Pretoria (see Jacobsz et al. 2014) to study the propagation of a zone of influence. The centrifuge model is illustrated in Figure 1. It comprised a frame manufactured from aluminium channel sections supporting an aluminium backing plate and a glass front containing a body of sand measuring 600 mm x 450 mm x 76 mm wide. Trapdoors of 50mm, 75mm or 100mm width could be accommodated in the base of the frame. The trapdoor was supported by a piston. The bottom compartment of the piston was filled with fluid that was extracted during tests by means of a second piston that was attached to a linear drive powered by a stepper motor. This system allowed the trapdoor to be lowered at a controlled rate. Sand was pluviated into the model from a sand hopper during which the flow rate and fall height were controlled to allow control over the placed density.

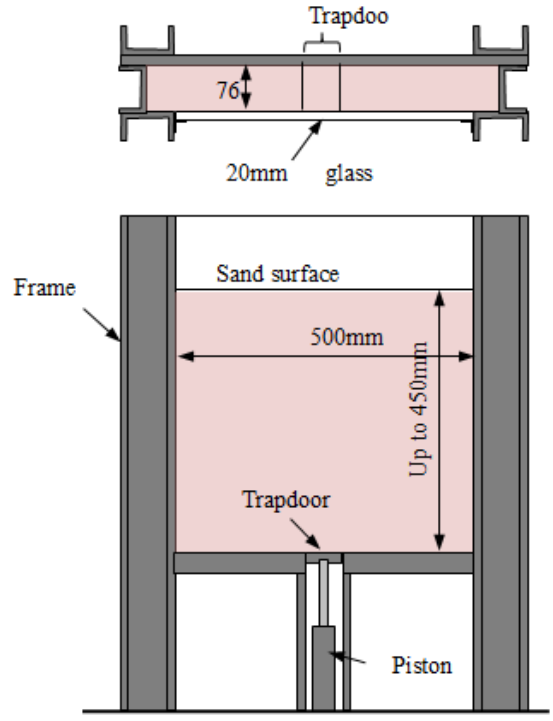

Figure 1. Illustration of the centrifuge model

3 FINITE ELEMENT MODELLING

3.1 Numerical method

The finite element method may be a helpful tool to use for simulating trapdoor experiments. However, it is difficult to simulate large deformation of trapdoors due to the numerical convergence problems caused by mesh distortion and the frictional contact between the soil and the strongbox.

The finite element formulations are based either on small deformations or using updated La-

grangian theory. In the Lagrangian formulation, an initial value ordinary differential equation for material evaluation at each Gauss point is solved by a time incremental scheme. Lagrangian formulations have been applied to many geotechnical applications and have proven to be robust and algorithmically easier to implement.

However, when the material deforms severely, elements becomes similarly distorted since mesh points are attached to material points in the Lagrangian description. The approximation accuracy of the elements then deteriorates, particularly for higher order elements, causing numerical instability (Belytschko et al. 2000). The Coupled Eulerian Lagrangian CEL approach (Benson 1992; Benson and Okazawa 2004) represents an attractive alternative. The results shown in this paper are obtained using the CEL method implemented in the commercial code Abaqus/Explicit (Dassault Systèmes 2017). In the CEL method, the Eulerian material is tracked as it flows through the mesh by computing its Eulerian volume fraction (EVF). Each Eulerian element is assigned a percentage, which represents the portion of that element filled with a material. If an Eulerian element is completely filled with a material, its EVF is 1; if there is no material in the element, its EVF is 0. The Lagrangian elements can move through the Eulerian mesh without resistance until they encounter an Eulerian element filled with material (EVF ≠ 0). A Lagrangian mesh is used to discretize the centrifuge model container, while a Eulerian mesh is used to discretize the soil.

3.2 Constitutive model

Triaxial testing for the sand used in the centrifuge has been performed. The measured triaxial peak angle of friction φ_p^{tr} is 42.3° and the measured critial state angle of friction φ_{cv} is 34.8°. It could be argued that plane-strain conditions are applicable to the centrifuge model, while the soil parameters are obtained using triaxial tests. Correlation between plane-strain and triaxial strength parameters are discussed by Bolton (1986) and Schanz and Vermeer (1996). Schanz and Vermeer (1996) have demonstrated that:

$$\varphi_p^{ps} \approx (5\ \varphi_p^{tr} - 2\ \varphi_{cv}\ )/3 \qquad (1)$$

where φ_p^{ps} is the plane-strain angle of friction.

Equation 1 gives a corresponding plane-strain angle of 47.2°. The plane strain and triaxial strain angles differ by about 5°. This is consistent with the observations of Schanz and Vermeer (1996) in dense sands.

In the finite element simulations, an improved Mohr-Columb criteria (see Potts and Zdravković 2004 for example) is adopted here to model the plastic behaviour of the soil in the finite element analysis. The angle of friction φ and the dilation angle ψ varies linearly with the plastic engineering shear strain $\varepsilon_s^p = \left|\varepsilon_1^p - \varepsilon_3^p\right|$ as shown in Figure 2.

Bolton's dilatancy equation is used to estimate the maximum angle of dilation ψ_{max}:

$$\varphi_p^{ps} - \varphi_{cv} = 0.8\,\psi_{max} \qquad (2)$$

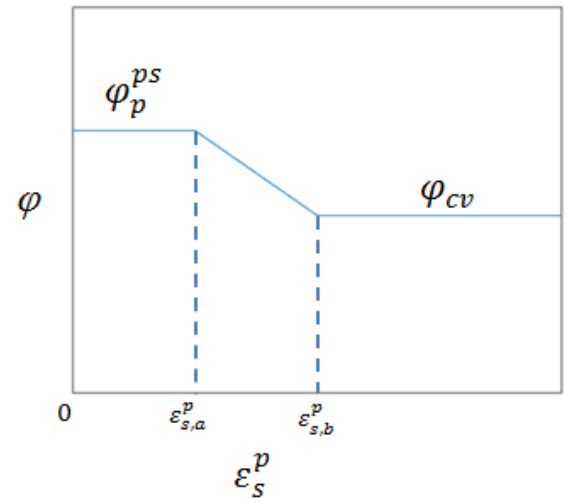

Figure 2. Hardening rule

The parameters used in the analysis are shown in Table 1.

Table 1. Parameters used in the analysis

Parameter	Value
Plane-strain peak angle of friction φ_p^{ps}	47.2°
Critical state angle of friction $\boldsymbol{\varphi_{cv}}$	34.8°
Maximum angle of dilation ψ_{max}	15.5°
Hardening parameter $\varepsilon_{s,a}^{p}$	0.05
Hardening parameter $\varepsilon_{s,b}^{p}$	0.2

3.3 Finite element model and geometry

The soil is modelled in an Eulerian domain. Three-dimensional (3D) linear brick hexahedron elements with reduced integration (element type: EC3D8R) are used to discretize the soil. Each Eulerian element has eight nodes and allows multiple materials to support the Eulerian transport phase. The geometry and the mesh of the finite element model are shown in Figures 3 and 4 (a), respectively. Due to the symmetry, only half of the whole model is considered in the 3D analysis. Only the base of the model container is modelled since the container is wide and the details of the side walls will have only a small effect on the dominating behaviour. Roller conditions are assumed at the outer vertical side and the central line. The vertical faces are constrained from moving in the normal direction. Full fixity boundary conditions are applied to the rigid model container. The sand layer has a height of H = 16.5 m and the trapdoor width is taken to be 2.5m. This corresponds to 330mm soil height and 50 mm trapdoor width (B) in the centrifuge tests with 50g acceleration. The interaction between soil and structures is calculated using the general contact algorithms in ABAQUS/Explicit. This contact algorithm incorporates finite-sliding formulation, which allows arbitrary motion of the surface.

4 RESULTS OF THE NUMERICAL MODELLING

4.1 Load-displacement of trapdoor

Displacement-control analyses were performed with a velocity of 0.013 m/s imposed on the trapdoor. The total displacement at the end of the analysis is 1.7 times the trapdoor width B. That is equivalent to 85mm in the centrifuge tests. Figure 4 (b) shows the flow of the soil. The reaction forces at the trapdoor is plotted against the trapdoor movement as shown in Figure 5.

The ordinate is the normalized ratio of the reaction forces (p) on the trapdoor to the initial reaction from overburden stress ($p_0=\gamma HA_T$, where A_T is the area of the trapdoor). The results show that stresses on the trapdoor reach a minimum at small displacements ($\Delta/B\approx0.05$) and then gradually increase. This pattern of load-displacement behaviour has also been observed in shallow trapdoors (Iglesia et al. 2009).

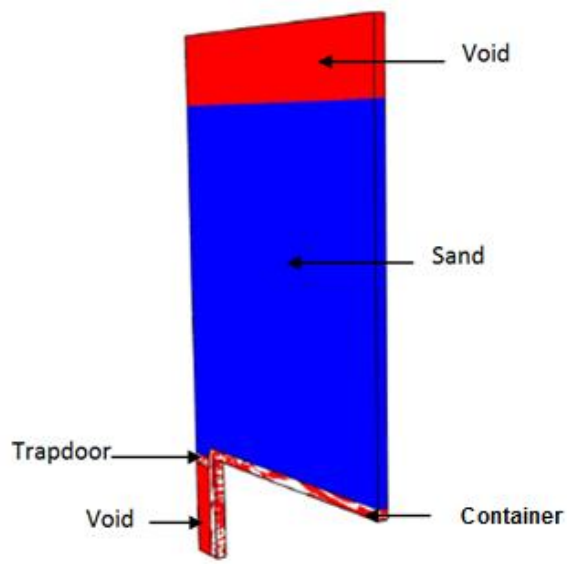

Figure 3. Geometry of the numerical model

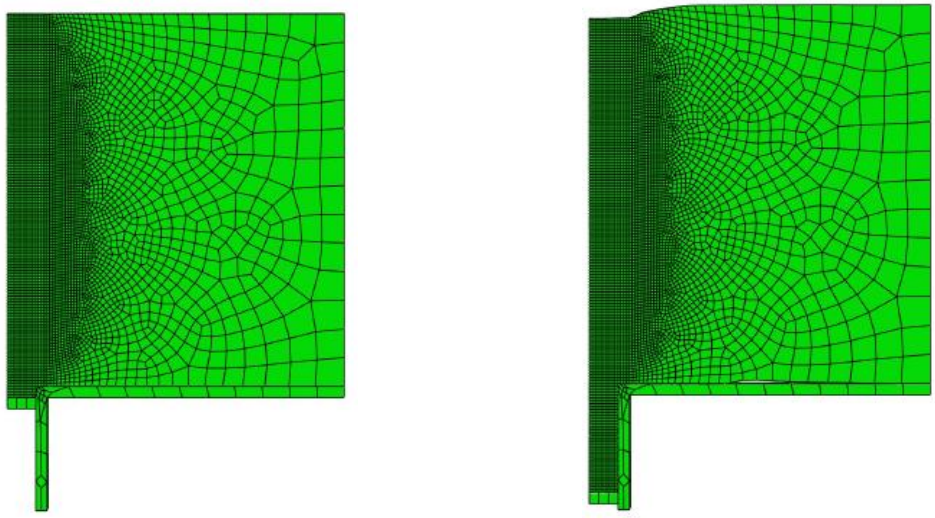

(a) (b)

Figure 4. Flow of the material: (a) at Δ/B=0 (b) at Δ/B=1.7

5 RESULTS OF THE NUMERICAL MODELLING

5.1 Load-displacement of trapdoor

Displacement-control analyses were performed with a velocity of 0.013 m/s imposed on the trapdoor. The total displacement at the end of the analysis is 1.7 times the trapdoor width B. That is equivalent to 85mm in the centrifuge tests. Figure 4 shows the flow of the soil. The reaction forces at the trapdoor is plotted against the trapdoor movement as shown in Figure 5.

The ordinate is the normalized ratio of the reaction forces (p) on the trapdoor to the initial reaction from overburden stress ($p_0=\gamma HA_T$, where A_T is the area of the trapdoor). The results show that stresses on the trapdoor reach a minimum at small displacement ($\Delta/B\approx0.05$) and then gradually increase. This pattern of load-displacement behaviour has also been observed in shallow trapdoors (Iglesia et al. 2009).

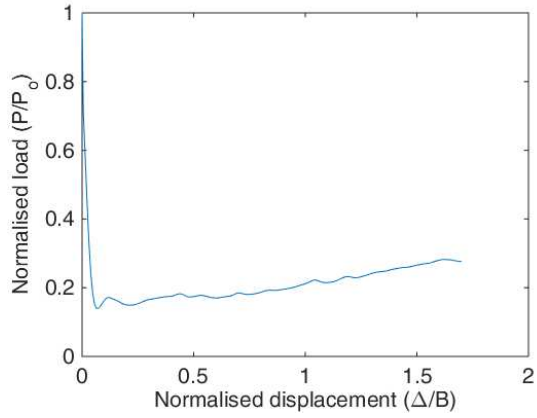

Figure 5. Trapdoor load-displacement curve

5.2 Propagation of shear bands

Figure 6 shows the propagation of the plastic engineering shear strain band above the trapdoor as it is being lowered. Failure surfaces initiate from the edges of the trapdoor, propagating upwards as shown in **Error! Reference source not found.** figure. The bands curve inwards under the influence of the mobilised dilation angle

which depends on the stress level and relative density of the placed soil (Bolton, 1986). Because the stress level is high as movement of the trapdoor first commences, a high dilation angle is mobilised, with the shear displacement steeply inclined from the vertical. As movement of the trapdoor continues, a second set of shear bands form suddenly and at a smaller angle to the vertical, reflecting the reduced dilation angle in response to a further reduction in stress. With large trapdoor movement, near vertical shear zones develop where the soil reaches critical state, and hence insignificant dilation, mobilises. The numerical results show good agreement with the patterns of behaviour observed in the centrifuge models (Figure 7).

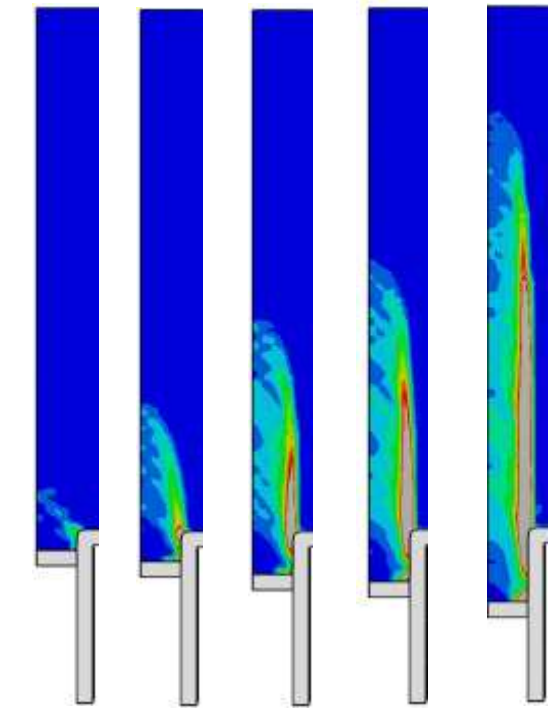

Figure 6. Propagation of plastic shear strain bands predicted by the finite element analysis: (a) Δ/B=0.05 (b) Δ/B=0.18 (c) Δ/B=0.37 (d) Δ/B=0.57 (e) Δ/B=0.74

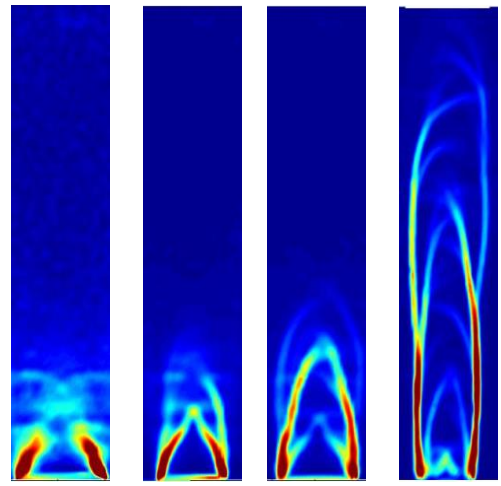

Figure 7. Propagation of shear strain bands in the centrifuge tests: (a) Δ/B=0.04 (b) Δ/B=0.12 (c) Δ/B=0.20 (d) Δ/B=0.80

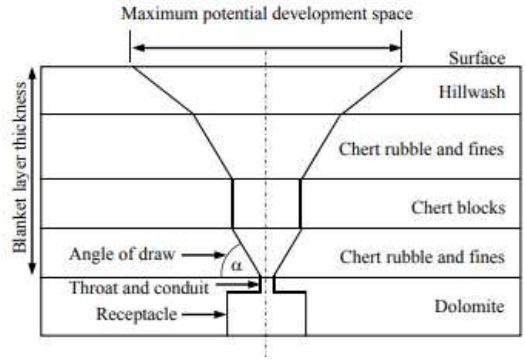

Figure 8. Estimation of the maximum potential development space of a sinkhole (modified from Buttrick & Van Schalkwyk 1995).

These results imply that the guidelines for the assessment of sinkhole size in South Africa are conservative and there is room for improving the current guidelines by adopting realistic mechanisms of sinkhole development. The South African National Standard for the development on dolomitic land SANS (2012) advocates that potential sinkhole size be assessed using a "rational approach" and presents a "deemed to satisfy" method taken from Buttrick & Van Schalkwyk

(1995). Buttrick & Van Schalkwyk (1995) proposed that the maximum potential development space for a sinkhole be estimated by extrapolating a funnel-shaped zone from a receptacle in or near bedrock towards the surface as shown conceptually in Figure 8.

6 CONCLUSIONS

In this paper, the CEL method is used to overcome the mesh distortion problem during numerical modelling of deep trapdoors subjected to large displacement. An improved Mohr-Coulomb model is used to describe the soil behaviour and the soil strength parameters obtained from triaxial testing are corrected for the plane-strain conditions exhibited in the centrifuge models. The numerical results show good agreement with the patterns of behaviour observed in the centrifuge models. These results imply that the current guidelines for the assessment of sinkhole size in South Africa are conservative, but that there is room for improvement.

7 ACKNOWLEDGEMENTS

The present work has been funded by the UK Royal Academy of Engineering (Grant Reference NRCP1516/1/42).

8 REFERENCES

Bolton, M.D. 1986. The strength and dilatancy of sands. Geotechnique **36**(1), 65-78.

Belytschko T, Liu W K, Moran B, 2000. Nonlinear Finite Elements for Continua and Structures, Wiley-Blackwell.

Benson, D.J. 1992. Computational methods in Lagrangian and Eulerian hydrocodes. Computer Methods in Applied Mechanics and Engineering, **99**(2–3): 235–394.

Benson, D.J., and Okazawa, S. 2004. Contact in a multi-material Eulerian finite element formulation. Computer Methods in Applied Mechanics and Engineering, 193(39–41): 4277–4298.Buttrick, D. & Van Schalkwyk, A. 1995. The method of scenario supposition for stability evaluation of sites on dolomitic land in South Africa. Journal of the South African Institution of Civil Engineering. Fourth quarter 1995: 9-14.

Costa, Y.D., Zornberg, J.G., Bueno, B.S. and Costa, C.L. 2009. Failure mechanisms in sand over a deep active trapdoor. ASCE Journal of Geotechnical and Geoenvironmental Engineering **135**(11), 1741-1753.

Dassault Systèmes. 2017. ABAQUS analysis user's manual. Simulia Corp., Providence, R.I.

Iglesia, G.R., Einstein, H.H. & Whitman, R.V. 2014. Investigation of soil arching with centrifuge tests. Journal of Geotechnical and Geoenvironmental Engineering **140**(2): 04013005

Jacobsz, S.W., Kearsley, E.P., Kock, J.H.L. 2014. The geotechnical centrifuge facility at the University of Pretoria. *Physical modelling in Geotechnics: Proceedings 8th ICPMG* (Eds: Gaudin, C. & White, D.), 169-174. CRC Press.

Koutsabeloulis, N. C., and Griffiths, D. V. (1989). Numerical modelling of the trapdoor problem. Geotechnique, **39**(1), 77–89.

Potts, D. M., and Zdravković, L. (1999). Finite element analysis in geotechnical engineering: theory, 1st edition, Thomas Telford Ltd., London.

South African Bureau of Standards. 2012. Development of dolomite land – Part 2: Geotechnical investigations and determinations. SANS 1936-2.

Schanz, T. & Vermeer, P. A. (1996). Angles of friction and dilatancy of sand. Geotechnique **46**(1): 145-151.

Stone, J.K. & Muir Wood, D. 1992. Effects of dilatancy and particle size observed in model tests on sand. Soils and Foundations **32**(4): 43-57.